Human Journals
Research Article
May 2020 Vol.:15, Issue:3

Glybatomaqtm312317b: Ab Initio Systematic Methodologies for Calculating Relative Solvation Free Energies of a Novel Series of Nano-Ligands [Nosunolin] Targeted the PHF20-Mediated Glioma and Glioblastoma Cell Apoptosis

Ioannis Grigoriadis*, Nikolaos Grigoriadis

Biogenea Pharmaceuticals Ltd., Thessaloniki, Greece.

Submission: 21 April 2020
Accepted: 29 April 2020
Published: 30 May 2020

www.ijsrm.humanjournals.com

Keywords: Glioma; Glioblastoma; Systematic parametrization; Polarizable force field; Quantum Chemistry

ABSTRACT

Free energy perturbation [FEP] ab initio quantum mechanics [QM] methods were developed for calculating relative salvation, treating the solute molecules and molecular mechanics [MM] for treating the surroundings are expected to enhance the speed and increase its use for drug design and lead optimization. Despite some success in applying QMMFEP methods to both computer-aided drug design and fragment-lead based optimization, QMMFEP calculations are rarely used in the drug discovery and pharmaceutical industry. Through the regulation of ETS1, it may play a role in angiogenesis, controlling endothelial cell motility and invasion. Future automation of the method and parallelization of the code for Linux 128/256/512 clusters is expected to execute electronic nose quantum noosphere improved quantum artificial fish docking algorithm application enhance the speed and increase its use for drug design and lead optimization. In this study, we introduce Glybatomaq, an ab initio systematic parametrization of polarizable force fields from quantum chemistry mechanics-based free energy perturbation method for calculating relative solvation free energies for systematic force field optimization on force-momentum-based self-guided Langevin dynamics with the ability to parametrize a wide variety of functional forms using flexible combinations of reference data. We outline several important challenges in force field development and how they are addressed in Force Balance, and present an example calculation where these methods are applied to understand what choice of the region S leads to the highest success probability in decision making from quantum information GlybatomaqTM superposition states Docking Algorithms in Transmission Mode Implementation of controlled quantum teleportation with an arbitrator for secure quantum channels via quantum dots inside enzyme cavities and development of a highly accurate polarizable novel Nano-ligand targeted the regulation of the ETS1, CASP8AP2 and FAS, LGI1, EPTP-ADAM22 Tudor domain of human PHF20-mediated Glioma and Glioblastoma cell apoptosis.

INTRODUCTION

Glioblastoma multiforme [GBM], which is classified by the World Health Organizations a grade IV glioma, exhibits a high morbidity and mortality, comprising 47.1% of all malignant tumors of the central nervous system [1,2]. In total, ~13,000 people in America are diagnosed with GBM each year [3]. The main treatment of GBM is surgical resection in combination with radiotherapy or chemotherapy. However, the majority of patients relapse within the 7 months following their original diagnoses [4]. Furthermore, resistance to current chemotherapy leads to a heavy tumor burden for patients with GBM. Although novel treatments, including immunotherapy and molecular targeted therapy, have been in development for several years [5,6], the 5-year survival rate is relatively low, with a median survival time of 15 months [4], indicating the urgency of determining novel therapies. Glioblastoma multiforme [GBM, WHO grade IV] is the most common and lethal subtype of primary brain tumor with a median overall survival of 15 months from the time of diagnosis. The Lindenbaum-Tarski algebra geometrically represented the modal equivalence classes with logical spaces in different ways under the equivalence relation and has been previously introduced as a 3D logical space subspaces allowing an automated vectorial representation in which anyone [of the eigenvalue statements] occupies a well-defined position on the equivalence classes and it is identified by a numerical ID when p and q are provably equivalent in T. This shows the application by factoring the algebra using decision procedures to quantum computing of formulas through the example of three coupled harmonic oscillators and proof assistants that allows pure mechanical computation both for generating algorithmic questions, rules and inferences. It is shown that this abstract formalism by this congruence relation can be geometrically represented with logical spaces and subspaces allowing a vectorial representation provided the logic is classical. MicroRNAs [miRNAs] are a class of small non-coding RNAs comprising ~19–23 nucleotides [7]. BiogenetoligandorolTM's uses the accuracy of electric charges plays an important role in protein–Glybatoma qTM™ligand docking, which is why QM-MM calculations are incorporated into docking procedures. Though Scheibe's austere formulation is remote from the normal practice of QM, it does not significantly differ from the functional interpretation implicit in normal practice. Fixed charges of Glybatoma qTM™ligands obtained from force-field parameterization are replaced by QM-MM calculations in the protein–Glybatoma qTM™ligand complex, treating only the Glybatoma qTM™ligand as the quantum region. BiogenetoligandorolTM's uses the QMMMIDD quantum thinking approach that provides unprecedented accuracy in fragment Glybatoma qTM™ligand based structure-based binding-energy calculations that enable formalistic application of QM methodologies to noncovalent hypergeometric and intra topology meta-Docking Interactions in complex systems as large as protein– Glybatoma qTM™ligand druggable complexes and conformational ensembles. BiogenetoligandorolTM's uses the accuracy of electric charges plays an important role in protein–Glybatoma qTM™ligand docking, which is why QM-MM calculations are incorporated into docking procedures. Though Scheibe's austere formulation is remote from the normal practice of QM, it does not significantly differ from the functional interpretation implicit in normal practice. Fixed charges of Glybatoma qTM™ligands obtained from force-field parameterization are replaced by QM-MM calculations in the protein–Glybatoma qTM™ligand complex, treating only the GlybatomaqTM™ligand as the quantum region. BiogenetoligandorolTM's uses the QMMMIDD quantum thinking approach that provides unprecedented accuracy in fragment Glybatoma qTM™ligand based structure-based binding-energy calculations that enable formalistic application of QM methodologies to noncovalent hypergeometric and intra topology meta-Docking Interactions in complex systems as large as protein– Glybatoma qTM™ligand druggable complexes and conformational ensembles. A PPI network was constructed using STRING [24], a database that provides functional interactions among proteins. Furthermore, eight genes of the miRNA associated DEGs were enriched in the glioma pathway, indicating their important roles in GBM. Each of the eight genes was targeted by more than one miRNA and one miRNA targeted more than one gene. miRNAs primarily exert effects via destabilization or translational repression by targeting the 3′ untranslated region of [1-24] mRNA transcripts in the cytoplasm [7].

MATERIALS AND METHODS

Molecular docking analysis and Drug discovery in BiogenetoligandorolTM Softwares.

Molecular docking between the proteins encoded by miRNA-associated DEGs and filtered chemicals was performed using BiogenetoligandorolTM [6-18]. Protein crystal structures [4-15] were downloaded from the Research Collaboratory for Structural Bioinformatics Protein Data Bank [PDB] [28] and chemical structures were obtained from PubChem [13-17]. The eight genes, including four that were upregulated and four that were downregulated [6-20] were submitted to the BiogenetoligandorolTM web tool as up and down tags to acquire [7-31] latent drugs in the therapy for GBM. First, the protein crystal structure was imported into [1-18] the BiogenetoligandorolTM 2.1.1 software on the BiogenetoligandorolTM interface

[13-50]. Compounds in the mol2 format were then imported into the software on the Docking interface and protein-ligand docking was run under the BiogenetoligandorolTM geom mode, after which a total score was exported, with these scores being directly proportional to the binding affinity.

Generation of a k-top scoring pairs classifier, Pearson R: correlation between the predicted and observed activity for the Glybatoma qTM test set.

For generating a classifier that is robust across gene expression technologies, BiogenetoligandorolTM takes a nonparametric approach to classification and adopts an extension of the top scoring pairs [TSP] method [7]. Using the R package ktspair [2-7], BiogenetoligandorolTM generates a k-top scoring pairs [k-TSP] classifier for predicting the status of the phenotype of interest on independent samples. The k-TSP algorithm is described in ANNEXIA-IIA, IIB Table Methods. [3-7], Other than above parameters, the robustness of developed model was also checked by Y-randomization [randomization of response] test. [19-23] This methodology helps to determine the robustness of a selected model and the significance of statistical results obtained. It requires a random scrambling of dependant variable [Y] of the training set molecules to produce new training sets those are dissimilar to the original [4-44].

Candidate Glybatoma qTM rank-based drug dentification.

BiogenetoligandorolTM connects gene expression changes associated with the phenotype of interest with candidate drug compounds that induce a negatively correlated [or “negatively connected”] gene expression profile. [19-44] BiogenetoligandorolTM compares the phenotype gene expression changes, termed a query signature, with rank-based gene expression profiles induced by BiogenetoligandorolTM compounds.

BiogenetoligandorolTM: Basic Concept: Molecular Dynamics, Monte Carlo Simulations, Langevin, Dynamics

Langevin dynamics ***is a system of x.i=vi, v.i=-mi-1 xiU(x)- γvi+σmi-1/2W.i.π(x,v)∝ e-βE(x,v)∝eβU(x)eβK(v),x.=v,v.=M\1U(x)γv+Σm1/2W.DKL*(p‖q)≡∫dxp(x)ln(p(x)q(x)).[x.v.]= *[v0] { R + [0 - M - 1 U (x)] { V + [0 - γ v + 2 γ (βM)1/2W.]{OeLΔt≈eLOVRVOΔt=eLOΔt2eLVΔt2eLRΔteLVΔt2eLOΔt2. R:eLRτ : [Δ x Δ v] = [v 0] τ V: e LV τ : [Δ x Δ v] = [0 - M - 1 U (x)] τ O:eLOτ:[ΔxΔv]=[0(a(τ)- 1)v+1-***

a(τ)2(βM)-1/2ξ]vk+1/4=vk-Δt2M1π;Λ⟨w⟩ρ;Λ)=12(⟨wshad⟩π;Λ⟨wshad⟩ρ;Λ),ω(x,v)≡ρx(x) π(v|x),DKL(ω|π)=∫dxdvω(x,v)ln[ω(x,v)π(x,v)] ∫dxdvρx(x)π(v/x) [37-49], ln[ρx(x)π(v/x)πx(x)π(v/x)]=∫dxρx(x)[∫dvπ(v|x)]ln[ρx(x) π x (x)] ∫ d x ρ x (x) l n [ρ x (x) π x (x)] = D K L (ρ x ‖ π x) DKL(ρx‖πx)=DKL(ω‖π)≈12(⟨wshad⟩π;Λ∼′-⟨wshad⟩π,Λ′;Λ∼′) =12(⟨wshad⟩π;Λ∼′-⟨wshad⟩ω;Λ∼′)=12(⟨wshad⟩π;Λ∼-⟨wshad⟩ ω;Λ∼) =12(⟨wshad⟩π;Λ-⟨wshad⟩ω;Λ) =12(⟨wshad⟩π⟨wshad⟩ω).ÃÃDKL(ρ‖π)=∫dxdvρ(x,v)ln[ρ(x,v)π(x,v)]=⟨ln[ρ(x,v)π(x,v)]⟩ρ = ⟨ l n [π (x , v) ⟨ e - w ⟩ x , v ; Λ ∼ π (x , v)] ⟩ ρ = ⟨ l n ⟨ e - w ⟩ x , v ; Λ ⟩ [39-50]

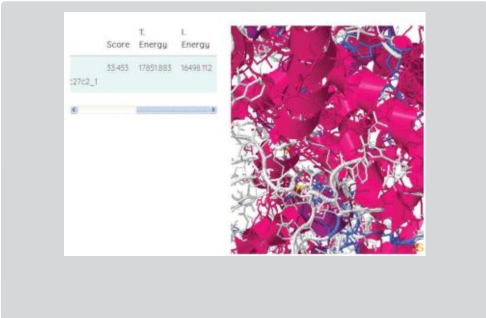

Figure No. 1: 3D Docking Interactions of the Glybatomaq TM5lge5d29a39e1317d within the Structure of Rbtumor suppress or bound to the trans activation do main of E2F2[PDB:1N4M].GlybatomaqTM_GlybatomaqTM_ligand_95f8bc27c2_1_run_20.lo,Model:1,T.Energy:17851.883,I.Energy:16498.112,vdW:16493.841,Coul:4.271, NumRotors:26,RMSD:6.169,Score:33.453,$Number_of_Clusters=10,$Seed=1985,$Leader_Info1[,Num_Members=33,Total_Energy=29218.194, vdW=28344.673, Coulomb=-0.687, Internal = 874.208].

Table No 1: 2D Structures and spectrum parameters of the GlybatomaqTM small molecule.

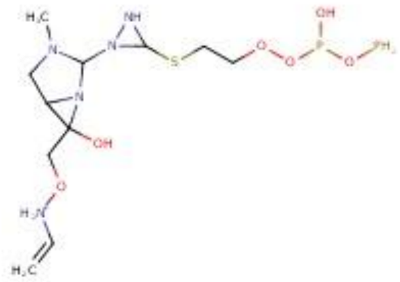	99	416.0917042	C=C[NH2+]OCC1[O]C2CN[C]C[N3NC3SCCOOP[O]OP]N21
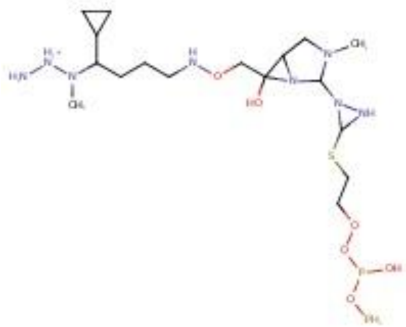	64	545.2183016	CN[[NH2+]N]C[CCCN OCC1[O]C2CN[C]C[N3NC 3SCCOOP[O]OP]N21]C1CC1
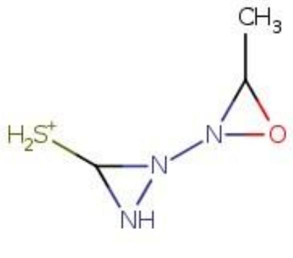	65	134.0382593	CC1ON1N1NC1[SH2+]

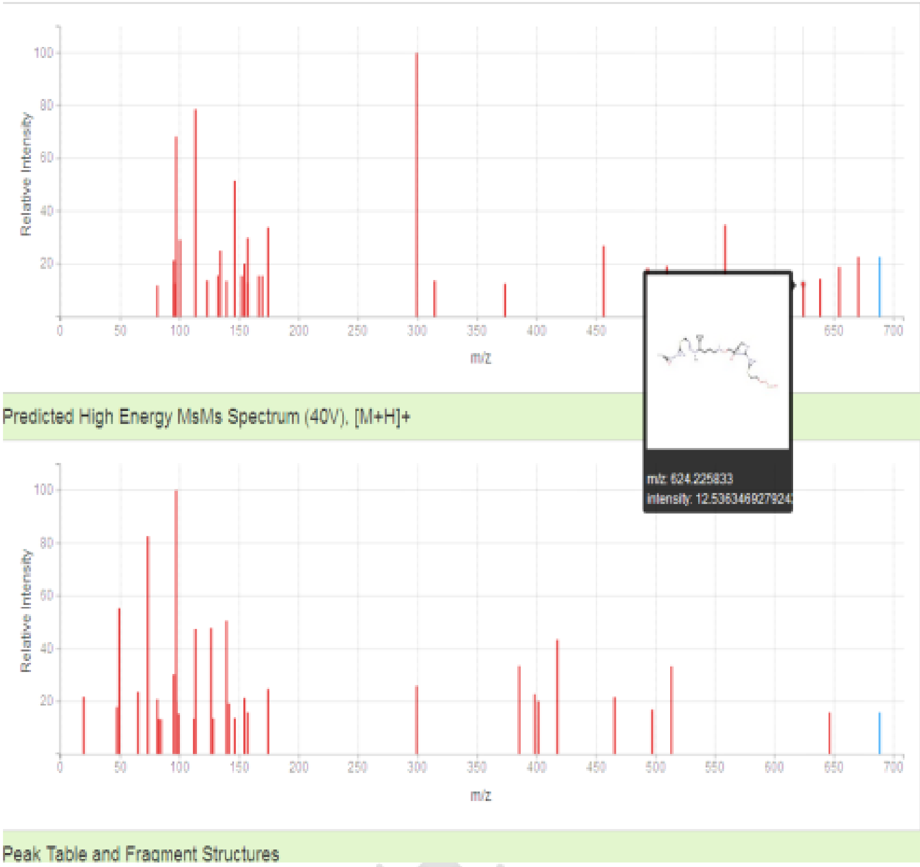

← Spectrum Prediction Input Parameters:

Parent Compound Structure [SMILES Format]	C1CCN=C[C1][C@@H]1C[C@@H][[C@H][C[=N1]C[=O]/N=C/1\CN=C[C@@H][[C@@H]1N1CCC[C @@H][C1]N]OC[C@@H][C[C@@H]1NN[CCN1N]/N=C/1\C[C@ @H][C[=O]N[C@]23C[C@@H][C[F][F]F]N3O2][C@@H][CC1]CCNN]OC]N][C@@H]1S[C@H][COC2=NO[C@@H][C[C@H]3C/C[=N/C]/[C@@H]4[C@H] [/C/3=N\C]NC=N4]C2]S1
Parent Compound Mass	1299.6569109198801
Spectra Type	ESI

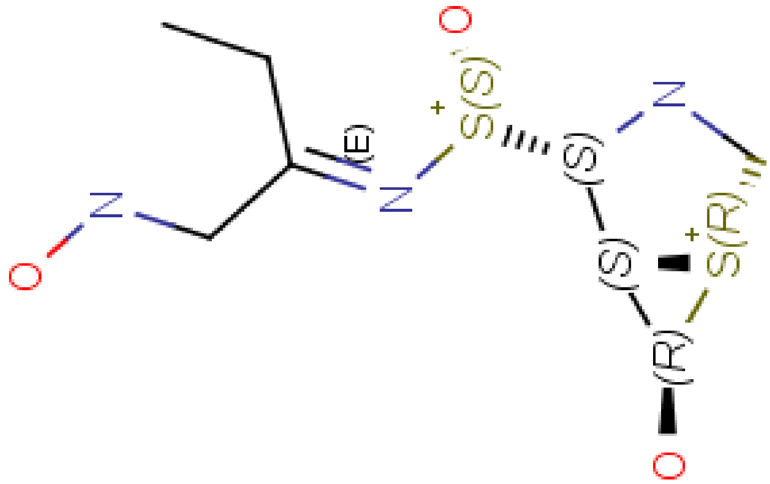

RESULTS AND DISCUSSIONS

In this study we find transformations between quantum reference frames, and show how the state, the dynamics, and the measurement change under these transformations. We show that the notion of entanglement and superposition are observer-dependent features, and we write the Schrödinger equation in quantum reference frames. Furthermore, we introduce a generalised notion of covariance of physical laws for quantum reference frames: ***E(H)=U(H⊕p⊕H¯⊕q)U† H¯ E(H)=V(H⊗P+H¯⊗Q)V† E~(H)=V~(H⊗P+H¯⊗Q)V~† E~(1)=P≤Δ(H')‖V~−V‖≤η‖H≤Δ'−E~(H)‖≤ϵH≤Δ'=P≤Δ(H')H'E~E~|ZH'(β)−(p+q)ZH(β)|(p +q)ZH(β)≤dm−ne−βΔ(p+q)e−β‖H‖+(eϵβ−1).Estate(N(ρ))=N'(Estate(ρ))+O(η),H'=H⊗|+y{ +H¯⊗|−y}|±y}=(|0{±i|1})/2ΔtΔE≥12Hmeas.'=cHmeas.e-iHmeas.Δt=Σje-iεjΔtεjεj,Hmeas.''= ΣjεjΔtmod2πεjεj Hmeas.'' Hmeas.'' Umeas.ψE0,0=ΣE',E''aE,E',E''ψE'E''θ(E,E',E''). δE·T(n)∈Ω1poly(n). H= Σi=0nσiz. UN,yx=x·ymodN0≤x<Nxotherwise HN,y=UN,y+UN,y† UN,ytUSEEMψE0,0=ψEΣE'aE'E',θ(E'),H=ΣjHj,H=Σi,jmAi,jai†aj+12ΣijBi,jaiaj+12Σi,jBj, i*ai†aj†A=A†,B=B† ai†,ai mn PrE'E-E'≤δE≥η. δE·T(n)∈1poly(n) {Hn}n=1∞ {Un}n=1∞ {Un}n=1∞ ΔE≤ηδE+21-ηH (1-e-m21-12η2,δE,mβ) ψt=2-n⁄2 Σy=12ny⊗Uty.*** We believe that the BiogenetoligandorolTMQMMID methods and the strategies developed here for a QM/polarized–MM implementation over the shell variables will be useful in the above equation to study more complex density functional theory DFT) based CPMD problems which is conventionally defined in catalysis, reactions in solid– liquid interfaces, crystallization on the Born–Oppenheimer surface. Dipole moments of the model compounds were also considered during optimization of the electrostatic parameters. Presented in

[Table1] is the QM dipole moments along with Drude and additive values. In general, the Drude values are in good agreement with the QM data. The differences with the additive model are systematically larger as expected given that the QM data was not considered when optimizing that model. We note that the impact of the dipole moment on interactions with the environment is less important with charged species vs. polar, neutral compounds as the monopole on the ions dominates such interactions. Here, for the first time we are introcuding the BiogenetoligandorolTM's drug design methodologies that use the accuracy of electric charges plays an important role in protein–GlybatomaqTM™ligand docking, which is why QM-MM calculations are incorporated into docking procedures. Though Scheibe's austere formulation is remote from the normal practice of QM, it does not significantly differ from the functional interpretation implicit in normal practice. Fixed charges of Glybatoma qTM™ ligands obtained from force-field parameterization are replaced by QM-MM calculations in the protein–Glybatoma qTM™ ligand complex, treating only the GlybatomaqTM™ligand as the quantum region. BiogenetoligandorolTM's uses the QMMMIDD quantum thinking approach that provides unprecedented accuracy in fragment Glybatoma qTM™ligand based structure-based binding-energy calculations that enable formalistic application of QM methodologies to noncovalent hyper geometric and intra topology meta-Docking Interactions in complex systems as large as protein– Glybatoma qTM™ ligand druggable complexes and conformational ensembles for the treatment of the glioma and glioblastoma cancer conditions.

Future Directions

Independently, the work-based estimate for ln[ρx[x]/π[x]] we used in the expensive lower bound [Table1] could be useful for other analyses. For example, an estimate of ln[ρx[x]/π[x]] could be used to interpret what features of x are most distorted by integrator bias, e.g., by checking which features of x are most predictive of extreme values of ln[ρx[x]/π[x]]. We also yield the two-dimensional Poisson distribution, about the derivation, is specific to the partition matching the integrable limit of the system, between configuration docking fitness scoring degrees equals the distribution obtained from the complex Ginibre ensemble, of freedom and velocities. We could also use this method to measure the KL divergence over any subset S of the state variables z = [x, v], provided we can sample from the conditional distribution for the complementary subset S of the state variables: π[zS |zS].

REFERENCES

1. Allen NJ, Barres BA (2009) Neuroscience: Glia more than just brain glue. Nature 457(7230): 675-677.
2. Lathia JD, Mack SC, Mulkearns-Hubert EE, Valentim CLL, Rich JN (2015) Cancer stem cells in glioblastoma. Genes Dev 29: 1203-1217.
3. Sanai N, Alvarez-Buylla, Berger MS (2005) Neural stem cells and the origin of gliomas. N Engl J Med 353(8): 811-822.
4. Lim DA, Cha S, Mayo MC, Chen MH, Keles E, et al. (2007) Relationship of glioblastoma multiforme to neural stem cell regions predicts invasive and multifocal tumor phenotype. Neuro Oncol 9(4): 424-429.
5. Goffart N, Kroonen J, Rogister B (2013) Glioblastoma-initiating cells: relationship with neural stem cells and the micro-environment. Cancers 5(3): 1049-1071.
6. Louis DN, Perry A, Reifenberger G, Von Deimling A, Figarella-Branger D, et al. (2016) The 2016 World Health Organization classification of tumors of the central nervous system: A summary. Acta Neuropathol 131(6): 803-820.
7. Laplante M, Sabatini DM (2012) mTOR signaling in growth control and disease. Cell 149(2): 274-293.
8. Mayer C, Zhao J, Yuan X, Grummt I (2004) mTOR-dependent activation of the transcription factor TIF-IA links rRNA synthesis to nutrient availability. Genes & Development 18(4): 423-434.
9. Kantidakis T, Ramsbottom BA, Birch JL, Dowding SN, White RJ (2010) mTOR associates with TFIIIC, is found at tRNA and 5S rRNA genes and targets their repressor Maf1. Proc Natl Acad Sci USA 107(26): 11823-11828.
10. O Reilly KE, Rojo F, She QB (2006) mTOR inhibition induces upstream receptor tyrosine kinase signaling and activates Akt. Cancer Res 66(3): 1500-1508.
11. Peterson TR, Sengupta SS, Harris TE (2011) mTOR complex 1 regulates lipin 1 localization to control the SREBP pathway. Cell 146(3): 408-420.
12. Ben-Sahra I, Hoxhaj G, Ricoult SJH, Asara JM, et al. (2016) mTORC1 induces purine synthesis through control of the mitochondrial tetrahydrofolate cycle. Science 351(6274): 728-733.
13. Jung CH, Jun CB, Ro SH (2009) ULK-Atg13-FIP200 complexes mediate mTOR signaling to the autophagy machinery. Molecular Biology of the Cell 20(7): 1992-2003.
14. Koren I, Reem E, Kimchi A (2010) DAP1, a novel substrate of mTOR, negatively regulates autophagy. Curr Biol 20(12): 1093-1098.
15. Peña-Llopis S, Vega-Rubin de Celis S, Schwartz JC (2011) Regulation of TFEB and V-ATPases by mTORC1. EMBO J 30(16): 3242-3258.
16. Settembre C, Zoncu R, Medina DL (2012) A lysosome-to-nucleus signalling mechanism senses and regulates the lysosome via mTOR and TFEB. EMBO J 31(5): 1095-1108.
17. Sarbassov DD, Ali SM, Sengupta S (2006) Prolonged rapamycin treatment inhibits mTORC2 assembly and Akt/PKB. Mol Cell 22(2): 159-168.
18. Sarbassov DD, Guertin DA, Ali SM, Sabatini DM (2005) Phosphorylation and regulation of Akt/PKB by the rictor-mTOR complex. Science 307(5712): 1098-1101.
19. Gan X, Wang J, Wang C (2012) PRR5L degradation promotes mTORC2- mediated PKC-δ phosphorylation and cell migration downstream of Gα12. Nat Cell Biol 14(7): 686-696.
20. Li X, Gao T (2014) mTORC2 phosphorylates protein kinase Cζ to regulate its stability and activity. EMBO Reports 15: 191-198.
21. Thomanetz V, Angliker N, Cloëtta D (2013) Ablation of the mTORC2 component Rictor in brain or Purkinje cells affects size and neuron morphology. J Cell Biol 201(2): 293-308.
22. García-Martínez JM, Alessi DR (2008) mTOR complex 2 (mTORC2) controls hydrophobic motif phosphorylation and activation of serum and glucocorticoid-induced protein kinase 1 (SGK1). Biochem J 416(3): 375-385.
23. Read RD, Cavenee WK, Furnari FB, Thomas JBA (2009) Drosophila model for EGFR-Ras and PI3K-dependent human glioma. PLoS Genetics 5(2): e1000374.
24. Bashir T, Cloninger C, Artinian N (2012) Conditional astroglial Rictor overexpression induces malignant glioma in mice. PLoS One 7(10): e47741.

25. Gulati N, Karsy M, Albert L, Murali R, Jhanwar-Uniyal M (2009) Involvement of mTORC1 and mTORC2 in regulation of glioblastoma multiforme growth and motility. Int J Oncol 35(4): 731-740.
26. Kohn AD, Summers SA, Birnbaum MJ, Roth RA (1996) Expression of a constitutively active Akt Ser/Thr kinase in 3T3-L1 adipocytes stimulates glucose uptake and glucose transporter 4 translocation. J Biol Chem 271(49): 31372-31378.
27. Morgan RA, Dudley ME, Wunderlich JR, Hughes MS, Yang JC, et al. (2006) Cancer regression in patients after transfer of genetically engineered lymphocytes. Science 314(5786): 126-129.
28. Gross G, Waks T, Eshhar Z (1989) Expression of immunoglobulin-T-cell receptor chimeric molecules as functional receptors with antibody-type specificity. Proc Natl Acad Sci USA 86(24): 10024-10028.
29. Eshhar Z, Gross G (1990) Chimeric T cell receptor which incorporates the anti-tumor specificity of a monoclonal antibody with the cytolytic activity of T cells: A model system for immunotherapeutical approach. Br J Cancer Suppl 10: 27-29.
30. Almåsbak H, Aarvak T, Vemuri MC (2016) CAR T Cell Therapy: A Game Changer in Cancer Treatment. J Immunol Res 2016: 1-10.
31. Golubovskaya V (2017) CAR-T cell therapy: From the bench to the bedside. Cancers 9(11): 150.
32. FDA Approves CAR-T Cell Therapy to Treat Adults with Certain Types of Large B-Cell Lymphoma.
33. Girolami M, Calderhead B (2011) Riemann manifold Langevin and Hamiltonian Monte Carlo methods. J R Stat Soc: Series B 73(2): 123- 214.
34. Wilkinson DJ (2006) Stochastic modelling for systems biology mathematical and computational biology, Chapman & Hall/CRC, London, UK.
35. Gelman A, Carlin JB, Stern HS, Rubin DB (2004) Bayesian data analysis, texts in statistical science. Chapman & Hall, CRC, London, UK.
36. Metropolis N, Rosenbluth AW, Rosenbluth MN, Teller AH, Teller E (1953) Equation of state calculations by fast computing machines. J Chem Phys 21(6): 1087-1092.
37. Kaderali L, Dazert E, Zeuge U, Frese M, Bartenschlager R (2009) Reconstructing signaling pathways from RNAi data using probabilistic Boolean threshold networks. Bioinformatics 25(17): 2229-2235.
38. Bois FY (2009) GNU MCSim: Bayesian statistical inference for SBML-coded systems biology models. Bioinformatics 25(11): 1453-1454.
39. Haario H, Laine M, Mira A, Saksman E (2006) Statistics and computing. DRAM: Efficient adaptive MCMC, Springer, Switzerland, pp. 339-354.
40. Brooks S, Gelman A, Jones GL, Meng XL (2011) Handbook of Markov chain Montecarlo. Handbooks of modern statistical methods. Chapman & Hall/CRC, London, UK.
41. Lawrence ND, Girolami M, Rattray M, Sanguinetti G (2010) Learning and inference in computational systems biology. Computational molecular biology, MIT Press, Massachusetts, Cambridge, London, England.
42. Rannala B (2002) Identifiability of parameters in MCMC Bayesian inference of phylogeny. Syst Biol 51(5): 754-760.
43. Duane S, Kennedy AD, Pendleton BJ, Roweth D (1987) Hybrid Monte Carlo. Phys Lett B 195(2): 216-222.
44. Radde N (2011) The role of feedback mechanisms in biological network models - a tutorial. Asian J Control 13(5): 597-610.
45. Calderhead B, Sustik M (2012) Sparse approximate manifolds for differential geometric MCMC. Adv Neural Inf Process Syst 26: 2888- 2896.
46. Rao CR (1945) Information and accuracy attainable in the estimation of statistical parameters. Bull Calc Math Soc 1(37): 235-247.
47. Calderhead B (2011) Differential geometric MCMC methods and applications. University of Glasgow, Scotland, UK.
48. Brooks S, Gelman A, Jones GL, Meng XL (2011) Handbook of Markov chain Montecarlo handbooks of modern statistical methods, Chapter 5. Chapman & Hall/CRC, London, UK.
49. Weckesser W (2008) Vfgen: A code generation tool. JNAIAM. 3(1-2): 151-165.
50. Wolff U (2004) Monte Carlo errors with less errors. Comput Phys Commun 156(2): 143-153